

# Optical optical double-resonance dual-comb spectroscopy with pump-intensity modulation

著者 (英)	Akiko Nishiyama, Yoshiaki Nakajima, Ken ' ichi Nakagawa, Atsushi Onae, Hiroyuki Sasada, Kaoru Minoshima
journal or publication title	Optics Express
volume	27
number	25
page range	37003-37011
year	2019-12-09
URL	<a href="http://id.nii.ac.jp/1438/00009339/">http://id.nii.ac.jp/1438/00009339/</a>

doi: 10.1364/OE.27.037003



# Optical–optical double-resonance dual-comb spectroscopy with pump-intensity modulation

AKIKO NISHIYAMA,<sup>1,2</sup> YOSHIAKI NAKAJIMA,<sup>1,2</sup>  KEN'ICHI NAKAGAWA,<sup>1</sup> ATSUSHI ONAE,<sup>2,3</sup> HIROYUKI SASADA,<sup>2,4</sup> AND KAORU MINOSHIMA<sup>1,2,\*</sup> 

<sup>1</sup>Department of Engineering Science, Graduate School of Informatics, University of Electro-Communications (UEC), 1-5-1 Chofugaoka, Chofu, Tokyo 182-8585, Japan

<sup>2</sup>Japan Science and Technology Agency (JST), ERATO MINOSHIMA Intelligent Optical Synthesizer (IOS) Project, 1-5-1 Chofugaoka, Chofu, Tokyo 182-8585, Japan

<sup>3</sup>National Metrology Institute of Japan (NMIJ), National Institute of Advanced Industrial Science and Technology (AIST), 1-1-1, Umezono, Tsukuba, Ibaraki, 305-8563, Japan

<sup>4</sup>Department of Physics, Faculty of Science and Technology, Keio University, 3-14-1, Hiyoshi Kohoku-ku, Yokohama 223-8522, Japan

\*k.minoshima@uec.ac.jp

**Abstract:** We apply an intensity-modulation technique to dual-comb spectroscopy to improve its detection sensitivity. The scheme is demonstrated via Doppler-free optical–optical double-resonance spectroscopy of Rb by modulating the intensity of a pump laser with frequencies set at rates 3 times lower and 50,000 times higher than the difference in the repetition rates of the two frequency combs. The signal-to-noise ratios are enhanced by 3 and 6 times for slow and fast modulations, respectively, compared to those of conventional dual-comb spectroscopy without any intensity modulation. The technique is widely applicable to pump-probe spectroscopy with dual-comb spectroscopy and provides high detection sensitivity.

© 2019 Optical Society of America under the terms of the [OSA Open Access Publishing Agreement](#)

## 1. Introduction

Dual-comb spectroscopy has been extensively employed as a powerful spectroscopic technique in various fields such as precision molecular spectroscopy [1], remote sensing [2], and spectro-imaging [3]. Because it is a type of Fourier-transform spectroscopy based on the interference of two short optical pulses originating from frequency combs with slightly different repetition rates, it provides a broad spectral coverage in a short data acquisition time [4,5]. Moreover, owing to the frequency stability and narrow spectral modes of the well-controlled frequency combs, dual-comb measurements realize high-spectral resolution and excellent accuracy in frequency determination, which are far superior to those of conventional Fourier-transform infrared (FTIR) spectroscopy. Until now, the high-resolution of dual-comb spectroscopy has been demonstrated in different types of Doppler-free spectroscopy such as two-photon absorption spectroscopy [6–8], optical–optical double-resonance (OODR) spectroscopy [9], and saturated absorption spectroscopy [10]. These demonstrations indicate that Doppler-free dual-comb spectroscopy has advantages, in terms of a broad spectral coverage and short data acquisition time, over conventional Doppler-free spectroscopy using continuous-wave (cw) lasers with a comparable high resolution. However, dual-comb spectroscopy requires an appropriate integration time to obtain a sufficient signal-to-noise ratio (SNR) [11]; this is because the photon numbers of a comb mode are much smaller than those of cw lasers. To extend Doppler-free dual-comb spectroscopy to various molecules, it is important to enhance the SNR in a practical integration time. To this end, thus far, some techniques such as cavity-enhanced spectroscopy [12,13], fluorescence detection [6–8], multiplication of the comb repetition rates [14], and background-free detection using an interferometer [15] have been reported.

We propose the application of an intensity-modulation technique to OODR dual-comb spectroscopy. Our motivation is to introduce the sensitivity improvement in dual-comb applications including molecular spectroscopy for various species. However, in this paper, we apply the scheme to Doppler-free OODR dual-comb spectroscopy of Rb as the first demonstration with simple scheme, and prove the improvement in the detection sensitivity. The intensity of the pump laser is modulated at frequencies  $1/3$  and  $50000$  times of  $\Delta f_{\text{rep}}$ , where  $\Delta f_{\text{rep}}$  is the difference between the repetition rates of the two combs, and a background-free OODR signal is successfully extracted. The intensity modulation reduces the noise caused by the intensity fluctuations in the comb spectrum, thereby increasing the SNRs. This modulation method broadly combines pump-probe spectroscopy with dual-comb spectroscopy.

## 2. Principle of modulation spectroscopy in Doppler-free OODR dual-comb spectroscopy

Figure 1 illustrates the energy level scheme of Rb atoms associated with its OODR spectrum. First, a pump 780-nm cw laser with a relatively narrow linewidth optically excites a part of the atoms in the  $5S_{1/2}$   $F'' = 2$  level to the  $5P_{3/2}$   $F' = 3$  level, an intermediate level. Then, the transitions from the above intermediate level to some hyperfine levels in the  $4D_{5/2}$  and  $4D_{3/2}$  states are observed using a probe 1529-nm frequency comb (signal comb). The observed spectral lines have a sub-Doppler width because the optical excitation caused by the pump laser selects a specific velocity group of the atoms [16].

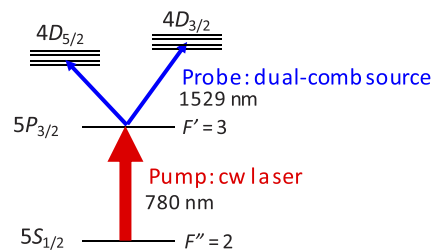


**Fig. 1.** Energy level scheme of OODR dual-comb spectroscopy of  $^{87}\text{Rb}$ . The pump cw laser frequency is stabilized to the hyperfine transition between the  $5S_{1/2}$  ( $F'' = 2$ ) and  $5P_{3/2}$  ( $F' = 3$ ) levels. A signal comb is used to probe some transitions from the intermediate level to the  $4D_{5/2}$  and  $4D_{3/2}$  levels with a sub-Doppler resolution.

To observe the transitions from the intermediate level, we perform dual-comb spectroscopy instead of conventional spectroscopy with a single-frequency cw source [17,18]. Dual-comb spectroscopy is a type of direct comb spectroscopy [19], in which one comb is used as the source for absorption spectroscopy, and the individual comb modes are separated using various devices such as a Fourier-transform spectrometer (FTS) [20], combination of a grating and virtually imaged phase array (VIPA) [21], and second comb (local comb). FTS and VIPA spectroscopy have been combined by some modulation techniques to improve the detection sensitivity, e.g., lock-in detection [22], noise-immune cavity-enhanced spectroscopy [23] and velocity modulation spectroscopy [24]. However, in dual-comb spectroscopy, the data acquisition is based on multi-heterodyne detection with a sampling frequency synchronized with the local comb repetition frequency; hence, it is not possible to apply a simple demodulation or lock-in detection with an arbitrary modulation frequency. Therefore, to apply a modulation technique in dual-comb spectroscopy, we set the intensity modulation frequency as  $\Delta f_{\text{rep}}/m$  or  $n\Delta f_{\text{rep}}$ , where  $m$  and  $n$  are positive integers and  $\Delta f_{\text{rep}}$  is the acquisition rate of the interferograms. A similar modulation frequency has been used in polarization-sensitive dual-comb spectroscopy [25].

Figure 2 illustrates the principle of OODR dual-comb spectroscopy with intensity modulation. We use two types of modulation: slow and fast modulations relative to  $\Delta f_{\text{rep}}$ , as shown in Fig. 2(a) and 2(b), respectively. The upper schematic traces in Fig. 2 are the temporal interferogram between the signal and local comb waves, presented in blue, and the modulated intensity of the pump laser, shown in red, in the time domain. In addition, the lower traces in Fig. 2 show the resulting dual-comb spectra in the radio-frequency (RF) domain. Note that the time and frequency are not scaled to the actual values.

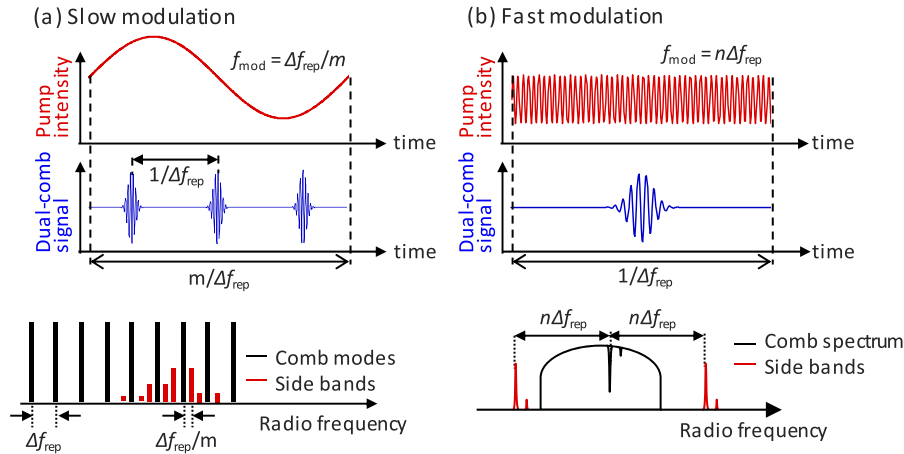


**Fig. 2.** Principle of intensity-modulated OODR dual-comb spectroscopy with slow modulation (a) and fast modulation (b). The upper traces are the temporal interferograms of the signal and local combs (blue) and pump laser intensity (red), and the lower traces are the RF comb spectra (black) and sideband spectra generated by the intensity modulation (red). (a) The intensity-modulation frequency is  $\Delta f_{\text{rep}}/m$ , where  $m = 3$ . The modulated signals appear at a frequency of  $\pm \Delta f_{\text{rep}}/m$  away from the RF comb modes. (b) The intensity-modulation frequency is  $n\Delta f_{\text{rep}}$ . In the lower trace, the modulated signals (red) appear at frequencies of  $\pm n\Delta f_{\text{rep}}$ , far away from the OODR absorptions in the comb spectrum (black).

For slow modulation, Fig. 2(a) shows the case with a modulation frequency ( $f_{\text{mod}}$ ) of  $\Delta f_{\text{rep}}/m$ , where  $m = 3$ , and three temporal interferograms are recorded for the period of the intensity modulation in the time domain. In the RF domain, the RF comb modes, shown in black, are equally spaced by  $\Delta f_{\text{rep}}$ . When the signal comb modes are tuned to an absorption frequency of a specific velocity group of atoms excited by the pump laser, then in the three interferograms, the intensity modulations of the pump laser induces intensity modulations of the comb modes. These modulations occur with the same period as the intensity modulation, i.e.,  $3/\Delta f_{\text{rep}}$ , in the time domain. In the RF domain, therefore, the modulations generate sidebands, as shown in red, separated by steps of  $\pm \Delta f_{\text{rep}}/3$  around a part of the RF comb modes associated with the probe transition. Because the generated sidebands, as shown in red, appear in the gap between the RF comb modes, as denoted in black, the extracted sidebands generate a background-free OODR spectrum.

We also apply a high-frequency modulation to OODR dual-comb spectroscopy with  $f_{\text{mod}}$  of  $n\Delta f_{\text{rep}}$ , as shown in Fig. 2(b). In general, a high frequency is preferred to remove the ubiquitous  $1/f$  noise [26]. In the RF domain, the black trace shows an envelope of the comb spectrum with sharp absorptions of OODR transitions. The sidebands generated by the intensity modulation, shown in red, appear at  $n\Delta f_{\text{rep}}$ , far from the OODR absorption. If  $n\Delta f_{\text{rep}}$  is sufficiently far, avoiding the comb spectral range, then a background-free OODR signal is obtained. In this

scheme, because we can separate the main body of the comb spectrum using an RF filter, saturation of the RF system is suppressed.

### 3. Experimental setup

Figure 3 shows the experimental setup for the Doppler-free OODR dual-comb spectroscopy with pump-intensity modulation. We use as the pump laser, an extended-cavity diode laser (ECDL) with a linewidth of less than 1 MHz at 780 nm. The absolute frequency of the ECDL is stabilized to the  $5S_{1/2} (F'' = 2) - 5P_{3/2} (F' = 3)$  hyperfine transition of  $^{87}\text{Rb}$  by using saturated absorption spectroscopy with a frequency modulation technique and lock-in detection. The dual-comb system consists of a signal comb and local comb, which are two homemade mode-locked Er-doped fiber lasers with center wavelengths of 1.5  $\mu\text{m}$  and slightly different repetition frequencies of approximately 56.6 MHz. The repetition frequency of the signal comb ( $f_{\text{rep,S}}$ ) and offset frequencies of both the combs are phase-locked to the RF signals referencing a global positioning system (GPS)-disciplined clock with an uncertainty of  $3 \times 10^{-12}$  in 1 s. Because the local comb mode is phase-locked to the signal comb mode by employing a high-bandwidth electric feedback via the cw laser, we achieve a narrow relative linewidth of the two combs that was sufficient to realize coherent averaging [27]. Details of the dual-comb setup are described in our previous paper [9]. Sub-Doppler resolution atomic spectroscopy have been performed using electro-optic phase modulator-based combs that have narrow spectral coverage and dense comb mode [28–30]. On the other hand, our fiber laser-based dual-comb system provides broadband spectral coverage and relatively small  $f_{\text{rep}}$  values, which has advantages in the application to high-resolution molecular spectroscopy and also wide applicability to other fields. The output of the signal comb is overlapped with that of the pump laser using a polarization beam splitter (PBS), and the beams are incident on the sample cell from the same direction. The sample cell is a 5-cm-long Rb gas cell heated to 70 °C and filled with  $^{85}\text{Rb}$  and  $^{87}\text{Rb}$  isotopes, which are mixed according to their natural abundances. The signal comb output is coupled with the local comb output by a fiber coupler and filtered by a band-pass filter (BPF) with a full-width at half maximum (FWHM) of 1.1 nm at approximately 1.53  $\mu\text{m}$ . In general, balanced detectors improve the SNR of measurements suppressing the detector saturation. But the improvement is not remarkable because of narrow spectral band width in our case. Thus, we employ a single photo detector (PD, New focus 1611). The signal from the photodetector is digitized synchronously at the repetition frequency of the local comb by a 14-bit digitizer.

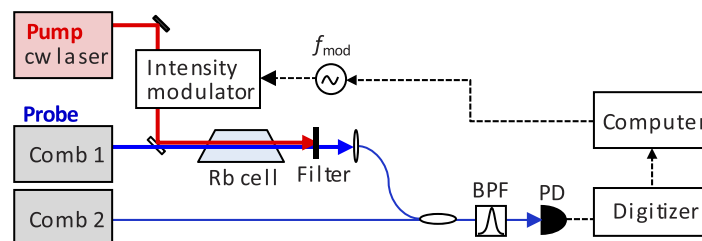


**Fig. 3.** Experimental setup for Doppler-free OODR dual-comb spectroscopy with intensity modulation. The frequency of the pump cw laser is related to the hyperfine transition between  $5S_{1/2} (F'' = 2) - 5P_{3/2} (F' = 3)$  of  $^{87}\text{Rb}$  using the same Rb cell as that for OODR spectroscopy. For slow modulation, the intensity modulator is an AOM, whereas an EOAM and a polarizer are used for fast modulation. PD: photodetector, BPF: optical band-pass filter.

The pump laser power is modulated by intensity modulators. When we adopt slow modulation, an acousto-optic modulator (AOM) is employed as the modulator. The zeroth order beam is used,

and the modulation depth is 0.81. In general, the response of AOM is fast enough also to drive several MHz modulation. However, an RF amplifier used as AOM driver has slow response in our setup; thus an electro-optic amplitude modulator (EOAM) and a polarizer are used for fast modulation. To modulate the population in the intermediate level, the EOAM is driven by a frequency of approximately 5 MHz, which is slower than the lifetime of the intermediate state [31]. The intensity-modulation depth after polarizer is 0.52. Higher modulation frequency than 5 MHz is applicable for other molecules with shorter life times. Taking the modulation frequency of  $f_{\text{rep}}/4$  avoids the overlap with sidebands and comb spectrum, and it maximizes the acquisition spectral range.

In both the cases, the peak intensity of the modulated pump laser light is set as that as averaging power of 1.0 mW. A function generator is used for driving the intensity modulators referencing the GPS-disciplined clock to provide accurate frequencies of  $\Delta f_{\text{rep}}/m$  and  $n\Delta f_{\text{rep}}$ . A systematic uncertainty attributed to the uncertainty of modulation frequency ( $\delta f_{\text{mod}}$ ) is derived as  $\delta f_{\text{mod}} \times f_{\text{rep}} / \Delta f_{\text{rep}}$ . This is negligible comparing to other uncertainties in absolute frequency determination in OODR dual-comb spectroscopy [9].

#### 4. Results and discussion

Figure 4(a) shows the Doppler-free OODR spectra of the  $5P_{3/2}(F=3) - 4D_{5/2}$  and  $4D_{3/2}$  transitions of  $^{87}\text{Rb}$  observed by the conventional dual-comb scheme without pump-intensity modulation. The  $\Delta f_{\text{rep}}$  was approximately 600 Hz, and the observed interferograms were coherently averaged over 1 min. To obtain a higher resolution than  $f_{\text{rep}}$ , the signal comb modes were scanned by varying  $f_{\text{rep},s}$  in 1-Hz increments. The equivalent scan step of the comb modes at 1530 nm was approximately 3.5 MHz. Following the measurement of the interleaved OODR dual-comb spectrum, reference spectra without the pump beam were recorded with the same averaging time and employed to obtain baselines for the normalization. In this measurement, the total measurement time including the reference measurement was 34 min. Figure 4(a) part (i) displays a wide range including the  $5P_{3/2}-4D_{5/2}$  and  $4D_{3/2}$  transitions of the normalized spectra, and Fig. 4(a) part (ii) and (iii) show the magnified views of the  $5P_{3/2}-4D_{5/2}$  and  $5P_{3/2}-4D_{3/2}$  transitions, respectively. The vertical blue lines and circles along the tops of the graphs denote the absolute frequencies of the hyperfine transitions [17]. In our OODR dual-comb spectroscopy, absolute transition frequencies are precisely determined with sub-MHz uncertainty as reported in our previous paper [9]. The hyperfine components of  $F=4$  and 3 of the  $4D_{5/2}$  state and  $F=3$  of the  $4D_{3/2}$  state are stronger than the other components. Because hyperfine transition intensities depend on the polarizations of the pump and probe beams [18], the observed hyperfine transition intensities with the orthogonally polarized pump and probe beams are different from those in our previous work [9], where we used parallel polarizations. The SNR of the spectrum is 56, where the SNR was calculated from the ratio of the absorption peak of the  $5P_{3/2}-4D_{5/2}$  transition and standard deviation of the background. The SNR was improved according to square root of the averaging time that was practically limited by robustness of frequency stabilization of the dual-comb system and pump cw laser. The dominant noise in this measurement is relative intensity noise (RIN) of dual-comb source [11,14]. Although the OODR spectra were normalized by the reference spectra, the intensity fluctuation of the dual-comb source degraded the SNR during the interleaving. The SNR in the range including the single transition with a few hyperfine splitting (Fig. 4(a) part (ii) and (iii)) is worse than cw laser measurements [32]. This is because the number of photons per spectral element are much smaller than cw laser due to the broadband spectral acquisition in dual-comb spectroscopy.

Figure 4(b) shows the obtained spectrum under application of the slow-intensity modulation. The  $\Delta f_{\text{rep}}$  was 600 Hz, and the modulation frequency,  $\Delta f_{\text{rep}}/m$ , was set as 200 Hz. We scanned the  $f_{\text{rep},s}$  similar to case of the conventional OODR dual-comb measurement. The averaging time for each  $f_{\text{rep},s}$  value was 2 min; thus, the total acquisition time was 34 min, which was the



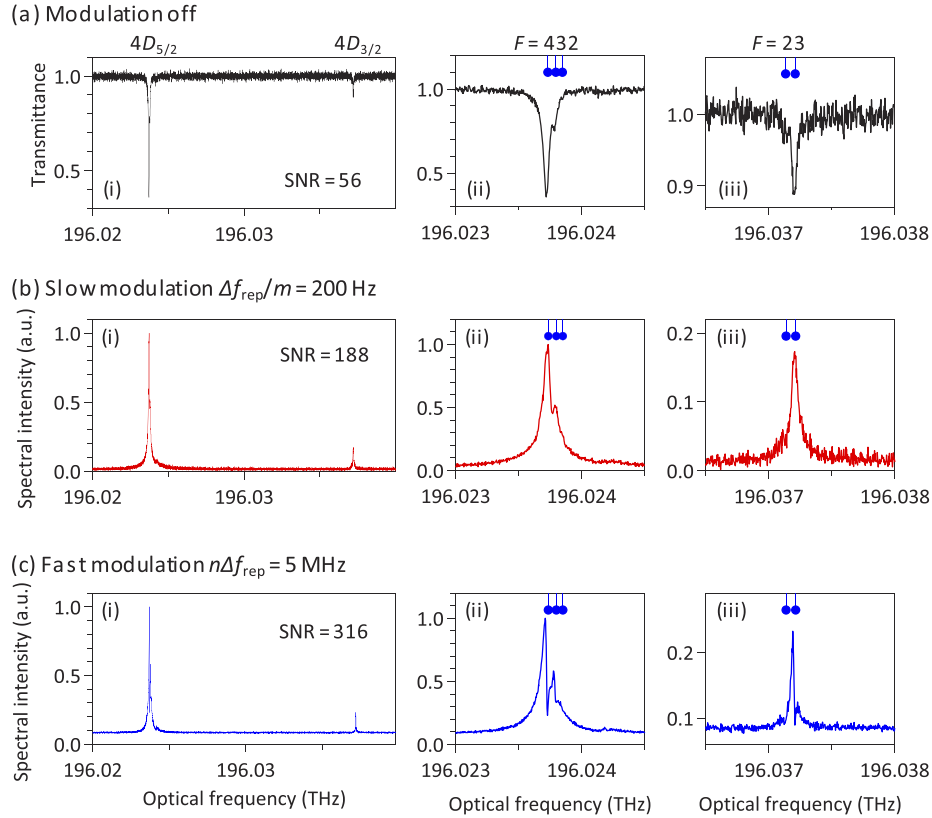


**Fig. 4.** Observed Doppler-free OODR dual-comb spectra of the  $5P_{3/2}$ - $4D_{5/2}$  and  $4D_{3/2}$  transitions employing (a) the conventional dual-comb setup, (b) slow-intensity modulation, and (c) fast-intensity modulation. In (a)–(c), each (i) shows a wide span including the range of 196.02–196.04 THz, and (ii) and (iii) show the magnified views around the transitions of  $5P_{3/2}$ - $4D_{5/2}$  and  $4D_{3/2}$ , respectively.

same as the acquisition time in the conventional OODR dual-comb measurement. To extract the background-free OODR signal from the resulting spectrum, two sidebands appearing at  $\pm\Delta f_{\text{rep}}/3$  from a real comb mode were averaged and divided by the comb mode intensity. The intensities of the sidebands were 20 times smaller at the absorption peak relative to the real comb modes. As shown in Fig. 4(b) part (i), we successfully obtained background-free OODR spectra, and the SNR was 188, which was approximately three times better than the SNR in the conventional OODR dual-comb measurement. The magnified views of the transitions are shown in Fig. 4(b) part (ii) and (iii). The transition peak frequencies show good agreement with conventional OODR dual-comb measurement. The spectral profile in the OODR spectrum is explained by the natural width and saturation of the intermediate state caused by the pump laser [18], which are well fitted with Lorentz functions. The full-width of half maximum of fitted Lorentz profile of the  $5P_{3/2}$  -  $4D_{5/2}$  ( $F=4$ ) line was 59.8 MHz in conventional dual-comb scheme modulation. However, the spectral widths in the slow-intensity modulation spectroscopy are broadened despite the peak intensity of the pump light being the same. Moreover, the spectral profiles are not well fitted with Lorentz functions. This broadening is caused by the harmonic terms of the modulation frequency. Also nonlinearity of the photodetector is considered as the origin of broadening. Since dual-comb spectroscopy is based on Fourier-transform spectroscopy, the nonlinearity does

not affect directly to line shapes. The nonlinearity of photodetector should be calibrated in time domain signal, but a simple calibration does not work perfectly as shown in ref [33].

Figure 4(c) shows the OODR spectra obtained by the fast-intensity modulation. We set  $\Delta f_{\text{rep}}$  as 100 Hz, so that it did not overlap the modulation signal with the real comb modes in the RF domain. We used modulation frequency  $n\Delta f_{\text{rep}}$  of 5 MHz, where  $n = 50000$ . As in the slow-modulation measurement, coherent averaging was performed over 2 min for each  $f_{\text{rep},s}$  value. The averaged interferogram was Fourier transformed, and we obtained a background-free OODR signal at a 5-MHz shifted frequency from the absorption. The sidebands were 10 times smaller than the real comb modes. The optical frequency shown in Fig. 4(c) was scaled considering the shift of 5 MHz in the RF domain. The SNR of the spectrum was 316, which was improved by 5.6 times than that in the conventional dual-comb measurement. The  $\Delta f_{\text{rep}}$  in this measurement was 6 times smaller than that in the conventional dual-comb measurement, i.e., the acquisition time of an interferogram was relatively 6 times longer. Therefore, the SNR improvement in the total averaging time was in disadvantage with a factor of square root of 6. However, despite the disadvantage caused by the measurement parameter setting, it achieved a remarkable SNR improvement. The magnified views in Fig. 4(c) part (ii) and (iii) show spectral profiles that are not simple absorption shapes. When the resonance conditions of the three levels are fulfilled, the probe signal comb has additional modes at frequencies of  $f_s \pm f_{\text{mod}}$ , which are attributed to a four-wave mixing process with the modulated pump beam. Above,  $f_s$  is the frequency of the signal comb mode at the resonant frequency. This four-wave mixing process is well known and studied for modulation transfer spectroscopy [34,35]. In this case, the line shapes observed at the shifted frequency change dramatically owing to the interference between the components caused by modulation of intermediate level population and Raman coherence. Additionally, as the cause of the broadening near the baseline, the effect of the nonlinearity of the detector should be also considered as in the case with slow modulation.

## 5. Conclusion

In conclusion, we demonstrated for the first time the application of intensity-modulation spectroscopy to dual-comb spectroscopy. We successfully acquired the modulation signals separated from the real comb mode signal by setting the modulation frequency as an integer ratio of  $\Delta f_{\text{rep}}$ . The intensity-modulation technique removed the intensity noise of the dual-comb source and showed a potential of sensitivity enhancement; three and six times improvements in the SNR were achieved by the slow and fast-intensity modulation schemes, respectively. The setup for intensity modulation scheme in dual-comb can be extend to frequency modulation spectroscopy using the same modulation frequency setup. In addition, it is applicable to double-resonance spectroscopy for various molecules, also to various other types of dual-comb spectroscopy such as pump-probe spectroscopy [36], laser-induced plasma spectroscopy [37] applying the modulation to the excitation of plasma, and velocity modulation spectroscopy [24] applying a specified modulation frequency to the discharge modulation. The modulation spectroscopy scheme is an excellent method to improve the sensitivity and expand the possibility of application of dual-comb spectroscopy.

## Funding

Japan Science and Technology Agency (JST), Exploratory Research for Advanced Technology (ERATO), MINOSHIMA Intelligent Optical Synthesizer (IOS) Project (JPMJER1304); Japan Society for the Promotion of Science (16J02345, 17K14435).



## Acknowledgments

We thank Hajime Inaba and Sho Okubo (AIST) for their valuable advice concerning the dual-comb system setup, and Masaaki Hirano, Yoshinori Yamamoto, and Takemi Hasegawa of Sumitomo Electronics Inc. for providing us the highly nonlinear fibers.

## Disclosures

The authors declare that there are no conflicts of interest related to this article.

## References

1. S. Okubo, K. Iwakuni, H. Inaba, K. Hosaka, A. Onae, H. Sasada, and F.-L. Hong, "Ultra-broadband dual-comb spectroscopy across 1.0–1.9  $\mu\text{m}$ ," *Appl. Phys. Express* **8**(8), 082402 (2015).
2. G. Ycas, F. R. Giorgetta, K. C. Cossel, E. M. Waxman, E. Baumann, N. R. Newbury, and I. Coddington, "Mid-infrared dual-comb spectroscopy of volatile organic compounds across long open-air paths," *Optica* **6**(2), 165 (2019).
3. T. Ideguchi, S. Holzner, B. Bernhardt, G. Guelachvili, N. Picqué, and T. W. Hänsch, "Coherent Raman spectro-imaging with laser frequency combs," *Nature* **502**(7471), 355–358 (2013).
4. I. Coddington, W. C. Swann, and N. R. Newbury, "Coherent multiheterodyne spectroscopy using stabilized optical frequency combs," *Phys. Rev. Lett.* **100**(1), 013902 (2008).
5. I. Coddington, N. Newbury, and W. Swann, "Dual-comb spectroscopy," *Optica* **3**(4), 414–426 (2016).
6. T. W. Hänsch and N. Picqué, "Laser Spectroscopy and Frequency Combs," *J. Phys.: Conf. Ser.* **467**(1), 012001 (2013).
7. A. Nishiyama, Y. Nakajima, K. Nakagawa, and K. Minoshima, "Precise and highly-sensitive Doppler-free two-photon absorption dual-comb spectroscopy using pulse shaping and coherent averaging for fluorescence signal detection," *Opt. Express* **26**(7), 8957–8967 (2018).
8. S. A. Meek, A. Hipke, G. Guelachvili, T. W. Hänsch, and N. Picqué, "Doppler-free Fourier transform spectroscopy," *Opt. Lett.* **43**(1), 162–165 (2018).
9. A. Nishiyama, S. Yoshida, Y. Nakajima, H. Sasada, K. Nakagawa, A. Onae, and K. Minoshima, "Doppler-free dual-comb spectroscopy of Rb using optical-optical double resonance technique," *Opt. Express* **24**(22), 25894–25904 (2016).
10. N. Kuse, A. Ozawa, I. Ito, and Y. Kobayashi, "Dual-comb saturated absorption spectroscopy," in *Conference on Lasers and Electro Optics* (Optical Society of America, 2013), paper CTu2I.1.
11. N. R. Newbury, I. Coddington, and W. Swann, "Sensitivity of coherent dual-comb spectroscopy," *Opt. Express* **18**(8), 7929–7945 (2010).
12. B. Bernhardt, A. Ozawa, P. Jacquet, M. Jacquy, Y. Kobayashi, T. Udem, R. Holzwarth, G. Guelachvili, T. W. Hänsch, and N. Picqué, "Cavity-enhanced dual-comb spectroscopy," *Nat. Photonics* **4**(1), 55–57 (2010).
13. A. J. Fleisher, D. A. Long, Z. D. Reed, J. T. Hodges, and D. F. Plusquellic, "Coherent cavity-enhanced dual-comb spectroscopy," *Opt. Express* **24**(10), 10424–10434 (2016).
14. A. Nishiyama, S. Yoshida, T. Hariki, Y. Nakajima, and K. Minoshima, "Sensitivity improvement of dual-comb spectroscopy using mode-filtering technique," *Opt. Express* **25**(25), 31730–31738 (2017).
15. T. Tomeberg, A. Muraviev, Q. Ru, and K. L. Vodopyanov, "Background-free broadband absorption spectroscopy based on interferometric suppression with a sign-inverted waveform," *Optica* **6**(2), 147 (2019).
16. W. Demtröder, *Laser Spectroscopy*, 4th ed. (Springer, 2008), Vol. 2.
17. W.-K. Lee and H. S. Moon, "Measurement of absolute frequencies and hyperfine structure constants of  $4D_{5/2}$  and  $4D_{3/2}$  levels of  $^{87}\text{Rb}$  and  $^{85}\text{Rb}$  using an optical frequency comb," *Phys. Rev. A* **92**(1), 012501 (2015).
18. H. S. Moon, L. Lee, and J. B. Kim, "Double-resonance optical pumping of Rb atoms," *J. Opt. Soc. Am. B* **24**(9), 2157 (2007).
19. N. Picqué and T. W. Hänsch, "Frequency comb spectroscopy," *Nat. Photonics* **13**(3), 146–157 (2019).
20. P. Maslowski, K. F. Lee, A. C. Johansson, A. Khodabakhsh, G. Kowzan, L. Rutkowski, A. A. Mills, C. Mohr, J. Jiang, M. E. Fermann, and A. Foltynowicz, "Surpassing the path-limited resolution of Fourier-transform spectrometry with frequency combs," *Phys. Rev. A* **93**(2), 021802 (2016).
21. S. A. Diddams, L. Hollberg, and V. Mbele, "Molecular fingerprinting with the resolved modes of a femtosecond laser frequency comb," *Nature* **445**(7128), 627–630 (2007).
22. J. Mandon, G. Guelachvili, and N. Picqué, "Fourier transform spectroscopy with a laser frequency comb," *Nat. Photonics* **3**(2), 99–102 (2009).
23. A. Khodabakhsh, C. A. Alrahman, and A. Foltynowicz, "Noise-immune cavity-enhanced optical frequency comb spectroscopy," *Opt. Lett.* **39**(17), 5034–5037 (2014).
24. L. C. Sinclair, K. C. Cossel, T. Coffey, J. Ye, and E. A. Cornell, "Frequency comb velocity-modulation spectroscopy," *Phys. Rev. Lett.* **107**(9), 093002 (2011).
25. K. A. Sumihara, S. Okubo, M. Okao, H. Inaba, and S. Watanabe, "Polarization-sensitive dual-comb spectroscopy," *J. Opt. Soc. Am. B* **34**(1), 154–158 (2017).

26. A. N. Dharamsi, "A theory of modulation spectroscopy with applications of higher harmonic detection," *J. Phys. D: Appl. Phys.* **29**(3), 540–549 (1996).
27. I. Coddington, W. C. Swann, and N. R. Newbury, "Coherent linear optical sampling at 15 bits of resolution," *Opt. Lett.* **34**(14), 2153–2155 (2009).
28. D. A. Long, A. J. Fleisher, D. F. Plusquellic, and J. T. Hodges, "Multiplexed sub-Doppler spectroscopy with an optical frequency comb," *Phys. Rev. A* **94**(6), 061801 (2016).
29. D. A. Long, A. J. Fleisher, D. F. Plusquellic, and J. T. Hodges, "Electromagnetically induced transparency in vacuum and buffer gas potassium cells probed via electro-optic frequency combs," *Opt. Lett.* **42**(21), 4430–4433 (2017).
30. D. A. Long, A. J. Fleisher, and J. T. Hodges, "Direct frequency comb saturation spectroscopy with an ultradense tooth spacing of 100 Hz," arXiv:1812.09342 (2018).
31. U. Volz and H. Schmoranzer, "Precision lifetime measurements on alkali atoms and on helium by beam-gas-laser spectroscopy," *Phys. Scr.* **T65**, 48–56 (1996).
32. M. Breton, P. Tremblay, C. Julien, N. Cyr, M. Têtu, and C. Latrasse, "Optically pumped rubidium as a frequency standard at 196 THz," *IEEE Trans. Instrum. Meas.* **44**(2), 162–165 (1995).
33. A. C. Johansson, L. Rutkowski, A. Filipsson, T. Hausmaninger, G. Zhao, O. Axner, and A. Foltynowicz, "Broadband calibration-free cavity-enhanced complex refractive index spectroscopy using a frequency comb," *Opt. Express* **26**(16), 20633–20648 (2018).
34. S. Le Boiteux, D. Bloch, and M. Ducloy, "Theory of optical heterodyne three-level saturation spectroscopy via collinear non-degenerate four-wave mixing in coupled Doppler-broadened transitions," *J. Phys.* **47**(1), 31–38 (1986).
35. Y. N. Martínez de Escobar, S. P. Álvarez, S. Coop, T. Vanderbruggen, K. T. Kaczmarek, and M. W. Mitchell, "Absolute frequency references at 1529 and 1560 nm using modulation transfer spectroscopy," *Opt. Lett.* **40**(20), 4731–4734 (2015).
36. A. Asahara and K. Minoshima, "Development of ultrafast time-resolved dual-comb spectroscopy," *APL Photonics* **2**(4), 041301 (2017).
37. J. Bergevin, T.-H. Wu, J. Yeak, B. E. Brumfield, S. S. Harilal, M. C. Phillips, and R. J. Jones, "Dual-comb spectroscopy of laser-induced plasmas," *Nat. Commun.* **9**(1), 1273 (2018).